

# UNIVERSITYOF BIRMINGHAM

### Research at Birmingham

# Horizontally acquired AT-rich genes in Escherichia coli cause toxicity by sequestering RNA polymerase

Lamberte, Lisa; Baniulyte, Gabriele; Singh, Shivani; Stringer, Anne M; Bonocora, Richard P; Stracy, Mathew; Kapanidis, Achillefs N; Wade, Joseph T; Grainger, David

10.1038/nmicrobiol.2016.249

Document Version Peer reviewed version

Citation for published version (Harvard):

Lamberte, LE, Baniulyte, G, Singh, SS, Stringer, AM, Bonocora, RP, Stracy, M, Kapanidis, AN, Wade, JT & Grainger, DC 2017, 'Horizontally acquired AT-rich genes in Escherichia coli cause toxicity by sequestering RNA polymerase', Nature Microbiology, vol. 2, 16249. https://doi.org/10.1038/nmicrobiol.2016.249

Link to publication on Research at Birmingham portal

#### **Publisher Rights Statement:**

Checked for eligibility: 03/08/2017
Lamberte, Lisa E., et al. "Horizontally acquired AT-rich genes in Escherichia coli cause toxicity by sequestering RNA polymerase." Nature microbiology 2.3 (2017): nmicrobiol2016249. doi:10.1038/nmicrobiol.2016.249

#### **General rights**

Unless a licence is specified above, all rights (including copyright and moral rights) in this document are retained by the authors and/or the copyright holders. The express permission of the copyright holder must be obtained for any use of this material other than for purposes permitted by law.

- Users may freely distribute the URL that is used to identify this publication.
- Users may download and/or print one copy of the publication from the University of Birmingham research portal for the purpose of private study or non-commercial research.
- User may use extracts from the document in line with the concept of 'fair dealing' under the Copyright, Designs and Patents Act 1988 (?)
- Users may not further distribute the material nor use it for the purposes of commercial gain.

Where a licence is displayed above, please note the terms and conditions of the licence govern your use of this document.

When citing, please reference the published version.

#### Take down policy

While the University of Birmingham exercises care and attention in making items available there are rare occasions when an item has been uploaded in error or has been deemed to be commercially or otherwise sensitive.

If you believe that this is the case for this document, please contact UBIRA@lists.bham.ac.uk providing details and we will remove access to the work immediately and investigate.

Download date: 01, Feb. 2019

#### ABSTRACT

Horizontal gene transfer permits rapid dissemination of genetic elements between individuals in bacterial populations. Transmitted DNA sequences may encode favourable traits. However, if acquired DNA has an atypical base composition, it can reduce host fitness. Consequently, bacteria have evolved strategies to minimise the harmful effects of foreign genes. Most notably, xenogeneic silencing proteins bind incoming DNA that has a higher AT-content than the host genome. An enduring question has been to understand why such sequences are deleterious. Here, we show that the toxicity of AT-rich DNA in Escherichia coli frequently results from constitutive transcription initiation within the coding regions of genes. Left unchecked, this causes titration of RNA polymerase and a global downshift in host gene expression. Accordingly, a mutation in RNA polymerase that diminishes the impact of AT-rich DNA on host fitness, reduces transcription from constitutive, but not activator-dependent, promoters.

#### INTRODUCTION

Bacteria obtain DNA from their environment by direct uptake (transformation), the action of viruses (transduction), or the acquisition of transmissible plasmids (conjugation)<sup>1</sup>. Thus, "horizontal" DNA transfer allows phenotypes to spread through bacterial populations. Transferred traits can be beneficial<sup>1</sup>. However, acquired sequences with a high AT-content may reduce host fitness<sup>2-6</sup>. Bacteria have developed mechanisms to diminish the toxicity of AT-rich genes. One approach involves a family of xenogeneic DNA binding proteins<sup>7,8</sup>. These proteins target DNA that has a higher AT-content than the host genome ("AT-rich" DNA), and silence transcription<sup>9-12</sup>. However, it is unclear why AT-rich DNA is toxic and why transcriptional silencing is beneficial.

The Histone-like Nucleoid Structuring (H-NS) protein of  $\gamma$ -proteobacteria is the best-characterised xenogeneic silencing protein  $^{9,13}$ . To reduce transcription, H-NS oligomerises across AT-rich genes  $^{9-12}$ . This process is triggered by nucleation at sequences containing a T:A step  $^{14-19}$ . Intriguingly, promoter  $^{-10}$  hexamers (consensus 5'-TATAAT-3', recognised by the RNA polymerase  $\sigma^{70}$  subunit) are excellent inducers of H-NS nucleation  $^{15,20}$ . Hence, H-NS can exclude RNA polymerase from, or trap RNA polymerase at, promoter DNA  $^{8,9,21,22}$ .

 A challenge has been to understand why horizontally acquired AT-rich DNA is toxic. As we noted previously, such regions contain a disproportionally high number of promoter-like sequences<sup>23-26</sup>. Furthermore, we showed that H-NS suppresses transcription primarily from promoters that are intragenic and/or far from gene starts<sup>25</sup>. Here, we test the hypothesis that transcription from intragenic promoters is a major cause of toxicity in cells lacking H-NS. Working with a sub-set of AT-rich genes, we demonstrate dramatic effects of H-NS on intragenic transcription. When this transcription is disabled, associated fitness costs decrease. Genome-wide, if derepressed, intragenic transcription sequesters RNA polymerase. This causes a global downshift in canonical gene expression.

Accordingly, a mutation in RNA polymerase that reduces transcription from constitutive promoters,

but not those that are activator-dependent, compensates for loss of H-NS.

69 70 71

68

#### RESULTS

- 72 *Identification of the canonical yccE promoter*
- We chose yccE as a model gene to understand xenogeneic silencing. We selected yccE because it is
- 74 AT-rich (66% A/T), silenced and bound by H-NS<sup>27</sup>, and contains at least two intragenic
- promoters<sup>25,28</sup>. Importantly, *yccE* can be studied in isolation because the adjacent genes are not H-NS
- bound (Figure 1a). We sought to understand the source of *yccE* transcription in cells lacking H-NS.
- As a starting point, we identified the canonical *yccE* promoter. We were aided by previous
- observations that yccE is a target for  $\sigma^{32}$  (heat shock  $\sigma$  factor)<sup>29</sup>. Segments of the yccE intergenic
- 79 region were fused to *lacZ* in reporter plasmid pRW50 (Figure S1a). Promoter activity located to a 55
- 80 base pair (bp) DNA fragment immediately upstream of yccE (Figure S1b). Figure 1b shows the
- sequence of this DNA fragment, named  $yccE\Delta 200$ . A  $\sigma^{32}$ -dependent promoter sequence is apparent.
- 82 We monitored transcripts produced from this promoter (PyccE) in vitro. To do this, fragments from
- the yccE intergenic region were cloned upstream of the  $\lambda oop$  terminator in plasmid pSR. Transcripts
- initiating at PyccE, and terminating at  $\lambda oop$ , should be ~106 nucleotides (nt) in length. Coincidentally,
- 85 the RNA-I transcript, derived from the pSR replication origin, is 108/107 nt long. To avoid confusing
- 86 transcripts, we first monitored RNAs produced using pSR without a PyccE insert. The data show that
- 87  $\sigma^{32}$  dependent synthesis of the RNA-I transcript is inefficient (Figure 1c, compare lanes 1 and 2).
- When the entire yccE intergenic region was cloned in pSR  $\sigma^{32}$  dependent yccE transcripts were
- 89 identified (Figure 1c, lane 3). The same transcripts were observed upon cloning the truncated
- 90  $yccE\Delta 200$  fragment (Figure 1c, lane 4). A 10 bp truncation at the 5' end of  $yccE\Delta 200$  abolished
- 91 transcription (Figure 1c, lane 5). To confirm correct identification of PyccE, DNA recognition
- elements for  $\sigma^{32}$  were mutated (detailed in Figure 1b). All mutations greatly reduced promoter activity
- 93 (Figure 1d).

94 95

- *Increased transcription of* yccE *in* ∆hns *cells does not require* PyccE
- 96 Convention dictates that PyccE should cause increased yccE transcription in cells lacking H-NS. We
- 97 considered this unlikely given the low activity, and  $\sigma^{32}$  dependence, of PyccE. Hence, we generated a
- 98 series of yccE::lacZ fusions to investigate the contribution of PyccE. The different constructs, labelled
- 99 *i* through *iv*, are illustrated below the graph in Figure 1e. We first measured *lacZ* expression in wild-
- type cells (Figure 1e, grey bars). When yccE was in the forward orientation, low-level lacZ expression
- was apparent. This was abolished upon deletion of PyccE (compare constructs ii and iii). In the
- reverse orientation, yccE stimulated higher lacZ expression (construct iv). This is consistent with our
- previous identification of a strong antisense promoter at the 5' end of yccE (adjacent to lacZ in this

- assay)<sup>28</sup>. Remarkably, in the absence of H-NS, *lacZ* expression increased in all scenarios (Figure 1e,
- white bars). This transcription must be due to intragenic promoters.
- 106 The yccE coding sequence is enriched for promoters
- A search identified 21 possible promoters within *yccE*. To test for function, we isolated promoters on
- 108 56 bp DNA fragments and fused them to *lacZ* (Figure 2a). Note that such sequences are too short to
- be subject to repression by H-NS<sup>25,30</sup>. Eleven DNA fragments stimulated β-galactosidase expression
- 110 twofold or more above background (labelled A-K in Figure 2a). Under the conditions of our
- experiment, 7 of the 11 intragenic promoters were more efficient at driving transcription than PyccE
- 112 (Figure 2a, black bar). Note that fragment "A" contains the strong antisense promoter described
- previously<sup>28</sup>.
- 114 Transcription initiation within yccE is repressed by H-NS in vitro
- In the context of the full *yccE* gene, intragenic promoters should be repressed by H-NS. We tested this
- in vitro using the pSR system. As noted above, with empty pSR, the 108/107 nt RNA-I transcript is
- produced. In addition, larger transcripts are generated from genes native to the plasmid. The complete
- set of transcripts produced from pSR is shown in Lane 1 of Figure 2b. In the figure, large (>1000 nt)
- pSR derived transcripts are highlighted by a black box and RNA-I is highlighted by a grey box. We
- introduced yccE into pSR, in either the forward or reverse orientation, upstream of the  $\lambda oop$
- terminator. Since yccE is 1257 bp in length, most intragenic transcripts should be separable from pSR
- derived transcripts. As expected, numerous transcripts between 100 and 1000 nt in length were
- detected for both *yccE* containing plasmids (compare Lanes 1, 2 and 6 in Figure 2b). For the plasmid
- containing yccE in the reverse orientation an additional small transcript was detected (highlighted by
- lower blue box in Figure 2b). This was expected, the transcript generated from the strong antisense
- promoter at the 5' end of yccE, has a size of 90 nt in this assay. Regardless of yccE orientation,
- addition of H-NS inhibited synthesis of most *yccE* derived transcripts (Lanes 3-5 and 6-9). Synthesis
- of the RNA-I transcript was enhanced by H-NS suggesting that RNA polymerase is titrated by
- promoters within *yccE*.
- 130 Intragenic promoters are the source of increased yecE transcription in cells lacking H-NS
- To confirm that H-NS repressed intragenic yccE promoters in vivo, we made derivatives of our
- 132 *yccE::lacZ* fusions. The derivatives carry mutations in intragenic -10 elements. Schematics are below
- the graph in Figure 2c. The open arrows show yccE lacking internal promoters. Full details are in
- Figure S2. In the absence of H-NS, the ability of mutated yccE alleles to stimulate lacZ expression
- was reduced (Figure 2c). Thus, both biochemical and genetic inspection show silencing of intragenic
- transcription by H-NS. We refer to this as "pseudo-regulation" that occurs independently of, and may
- be mistaken for, the control of mRNA synthesis. Thus, supposed gene regulatory effects of H-NS may
- often be due to intragenic promoters.

The fitness cost of yccE is a consequence of intragenic transcription

We predicted a link between intragenic transcription and reduced fitness associated with loss of H-NS. Hence, *E. coli* M182, and the *hns*::kan variant, were transformed with pSR carrying *yccE* with or without internal promoters. Importantly, *yccE* mRNA cannot be expressed in this scenario; no upstream promoter is present. We monitored cultures inoculated with these strains (Figure 2d,e). In all cases, cells lacking *hns* had reduced fitness compared to the parent. However, this fitness defect was smaller for the *yccE* derivative lacking internal promoters (Figure 2e). Complete elimination of the fitness defect was not expected; AT-rich genes present on the *E. coli* chromosome also contribute.

Repression of intragenic transcription by H-NS reduces the fitness cost of many AT-rich genes

We identified other solitary genes targeted by H-NS: yfdF, ykgH, yjgN and yjgL. We cloned these, and derivatives lacking intragenic promoters, upstream of the λοορ terminator in pSR. The fepE gene, which has an AT-content of 55%, was included as a control. The constructs are illustrated above the gel image in Figure 3a. Full gene sequences are in Figure S3. Figure 3a shows results of in vitro transcription experiments. Whilst RNA polymerase did not initiate transcription within fepE (Lane 1), intragenic transcription was observed for yfdF, ykgH, yjgN and yjgL (Lanes 2, 4, 6 and 8). Mutation of intragenic promoters reduced this transcription (Lanes 3, 5, 7 and 9). The coding regions described above were also cloned upstream of lacZ in pRW50 (Figure 3b). Expression of lacZ was measured in M182 or the hns::kan derivative (Figure 3b). Upon deletion of hns, expression of lacZ downstream of yfdF, ykgH, yjgN or yjgL, but not fepE, increased (solid arrows). In contrast, no such increase occurred when intragenic promoters were mutated (open arrows). These analyses are consistent with silencing of intragenic promoters by H-NS at all loci tested. Hence, we measured the fitness cost of multicopy yfdF, ykgH, yjgN and yjgL in cells with and without H-NS. In all cases, the fitness deficit between wild-type and hns::kan cells decreased upon mutation of intragenic promoters (Figure 3c,d). Furthermore, changes in fitness and lacZ expression were significantly correlated (Figure S4a).

AT-rich genes titrate RNA polymerase and cause a global downshift in housekeeping transcription

RNA polymerase levels are limited in *E. coli*<sup>31</sup>. Consequently, multiple copies of a strong promoter can hinder growth and titrate transcription of the *lac* operon (Figure S4b). Interestingly, RNA polymerase levels do not increase in cells lacking H-NS (Figure S5). Therefore, competition for the enzyme must increase; more promoters compete for a limited supply of RNA polymerase. Logically, migration of RNA polymerase to spurious promoters should cause a global downshift in canonical transcription. However, despite many studies of the H-NS controlled transcriptome, a universal downshift has never been reported<sup>9,10,27,32,33</sup>. We reasoned that this might result from data normalisation approaches used previously. Briefly, transcriptome analysis compares RNA levels in two strains. Comparison requires a point of reference believed to be consistent between the strains. For example, it may be assumed that housekeeping genes are similarly transcribed or that averaged

175 transcription across all genes will be equivalent. Problematically, these approaches cannot 176 differentiate between technical variation and genuine shifts in global transcription. To circumvent this 177 problem, spiked-in RNA standards can be used<sup>34</sup>. We adapted this tactic to quantify global effects of H-NS on transcription. Briefly, we grew E. coli MG1655, and the hns::kan variant, to mid-log phase. 178 179 We then counted colony-forming units for each E. coli culture. The same was done for a single culture 180 of Salmonella Typhimurium. Accordingly, we were able to mix a defined number of clonal 181 S. Typhimurium cells with each E. coli strain. The cell mixtures were subject to transcriptome 182 analysis. For identically grown S. Typhimurium cells, differences in RNA abundance must result from 183 processing variation. Hence, at the end of the procedure, transcripts mapping uniquely to S. Typhimurium were used to normalise the data. Figure 4a shows a post-normalisation plot of read 184 185 depth for each E. coli gene in each strain. The diagonal blue line shows the expected position of data 186 points if transcription is unchanged between strains. There is a downshift in transcription of genes not 187 bound by H-NS (black). Conversely, H-NS bound genes (red) are transcribed more frequently. This 188 behaviour is exemplified in Figure 4b.

- 189 RNA polymerase titration can be visualised directly
- Genes bound by H-NS are overrepresented near the chromosome replication terminus (Ter)<sup>35,36</sup>. 190
- Conversely, most RNA polymerase binds near the origin of replication (Ori)<sup>37</sup>. These loci occupy 191
- distinct intracellular territories; Ter typically frequents mid-cell whilst Ori migrates to the poles<sup>37-39</sup>. 192
- 193 Consequently, it should be possible to visualise titration of RNA polymerase at the cellular level.
- Previously, we used super resolution microscopy to track individual RNA polymerase molecules in 194
- live E. coli<sup>40</sup>. Here, we repeated this analysis to examine the effect of deleting hns. In wild-type cells, 195
- 196 RNA polymerase clusters near the quarter cell positions (Figure 4c, top). However, in cells lacking
- 197 H-NS, RNA polymerase is redistributed and mid-cell is occupied (Figure 4c, middle). Consistent with
- 198 unaltered RNA polymerase abundance, occupancy of mid-cell corresponds to reduced RNA
- 199 polymerase abundance elsewhere (Figure 4c).

200

- 201 RNA polymerase mutation can compensate for loss of H-NS by favouring regulated transcription
- An aspartic acid substitution in the RNA polymerase  $\sigma^{70}$  subunit (G424D in E. coli) can compensate 202 for loss of H-NS<sup>41</sup>. This side chain could clash with the promoter -10 element during transcription 203
- initiation<sup>41</sup>. According to our model, promoters within genes are constitutive; they rely solely on their 204
- 205 DNA sequence to bind RNA polymerase. Conversely, canonical promoters are regulated; a complex
- array of transcriptional activators stabilise RNA polymerase binding and DNA unwinding<sup>42</sup>. We 206
- 207 reasoned that transcriptional defects, due to the G424D mutation, might be more pronounced at
- constitutive promoters. To test this, we purified RNA polymerase containing  $\sigma^{70}$  or the G424D 208
- derivative. We then investigated the ability of the RNA polymerase derivatives to stimulate 209
- 210 unwinding of a promoter -10 element using KMnO<sub>4</sub> footprinting. The semi-synthetic NM501

promoter was used because it has constitutive activity, by virtue of a consensus -10 element, but can be upregulated by the transcriptional activator CRP<sup>43</sup>. The G424D mutation completely abolished DNA opening by RNA polymerase in the absence of CRP (Figure 4d, compare lanes 2-5 and 6-9). In contrast, when CRP was present, the  $\sigma^{70}$  G424D mutation had little effect (compare lanes 10-13 and 14-17). Similarly, *in vivo*, the  $\sigma^{70}$  G424D mutation caused transcriptional defects at 7 of 8 constitutive promoters (Figure 4e). However,  $\sigma^{70}$  G424D functioned as well as, or better than, wild type RNA polymerase at activator dependent promoters (Figure 4f).

218219

#### DISCUSSION

220 The AT-rich genes examined here impose a fitness cost due to intragenic promoters. This phenomenon is likely to be widespread in bacteria; functional homologues of H-NS are apparent in 221 diverse species<sup>8</sup>. Furthermore, the DNA binding properties of RNA polymerase are highly 222 223 conserved<sup>42</sup>. We suggest that misappropriation of cellular resources underlies the *hns* phenotype. 224 Redeployment of the finite RNA polymerase pool causes uniform suppression of canonical transcription. Whilst this general effect is likely to be pervasive, we do not exclude organism-specific 225 complications. For example, in Pseudomonas aeruginosa, loss of H-NS-like proteins causes prophage 226 induction and cell death<sup>44,45</sup>. Interestingly, linear H-NS filaments do not pose a barrier to transit of 227 RNA polymerase<sup>46</sup>. Accordingly, transcription of an mRNA, and silencing of intragenic promoters, 228 229 could occur simultaneously. For example, in this work, PyccE was active both in isolation and 230 upstream of H-NS bound yccE. We speculate that gene silencing by H-NS may have evolved to 231 discriminate between canonical and spurious RNA synthesis.

232233

#### MATERIALS AND METHODS

- 234 Strains, plasmids and general methods
- 235 E. coli JCB387 Δnir Δlac and MG1655 have been described previously<sup>47,48</sup>. M182hns::kan and
- 236 KF26hns::kan were constructed by P1 transduction of hns::kan from MG1655 into the respective
- parent strains. The MG1655 hns::kan strain was provided by Ding Jin. M182rpoD::kan was generated
- using gene doctoring according to the protocol of Lee et  $al^{49}$  using the plasmids and oligonucleotides
- listed in Table S1. Note that, prior to gene doctoring, M182 strains were transformed with plasmid
- pVR $\sigma$  that encodes  $rpoD^{50}$ . Quickchange mutagenesis was used to introduce the G424D mutation into
- pVR $\sigma$  encoded *rpoD* (Table S1). Fortuitously, chromosomal and plasmid encoded  $\sigma^{70}$  were produced
- 242 at indistinguishable levels (Figure S6). Sample sizes for all experiments were selected to ensure
- reproducibility in line with our previous work.
- 244 DNA fragments and gene expression assays
- 245 Promoter::lacZ fusions were made by cloning DNA fragments upstream of lacZ in the low copy
- number plasmid pRW50<sup>51</sup>. The nested deletions in the *yccE* intergenic region were generated by PCR

- and oligonucleotides shown in Table S1. The various yccE, yfdF, ykgH, yigN and yigL alleles were
- 248 synthesised by Invitrogen and some contain silent mutations to remove *Eco*RI or *Hin*dIII restriction
- sites to facilitate cloning (Figures S2a and S3). Oligonucleotides used to amplify the different alleles
- 250 for cloning into pSR and pRW50 are shown in Table S1. The 56 bp intragenic yccE fragments were
- 251 generated with overlapping oligonucleotides (Table S1). The resulting single stranded overhangs were
- 252 filled with DNA polymerase before cloning. β-galactosidase assays were done using the protocol of
- 253 Miller<sup>52</sup>. All assay values are the mean of three biological replicates and the error bars show standard
- deviation from the mean. Experiments were done at least twice. Cells were grown aerobically at 37°C,
- to mid-log phase, in LB media.
- 256 Bioinformatic analysis of genes and design of new coding regions
- Our stringent search criteria selected putative  $\sigma^{70}$  dependent promoters as described previously<sup>25</sup>.
- 258 Thus, sequences were selected that matched the motifs 5'-TAnAAT-3', 5'-TATnAT-3' or 5'-TATAnT-
- 3'. The relaxed search selected the sequence 5'-TAnnnT-3'. To inactivate promoter -10 elements the
- initial 5'-TA-3' was replaced with 5'-GG-3'
- 261 Proteins, KMnO<sub>4</sub> footprinting and in vitro transcription assays
- 262 H-NS and RNA polymerase were prepared as described previously<sup>53</sup>. DNA fragments for KMnO<sub>4</sub>
- 263 footprinting experiments were derived from Qiagen maxi-preparations of plasmid pSR. Thus,
- promoter DNA fragments were excised from pSR by sequential digestion with *Hin*dIII and then *Aat*II.
- After digestion fragments were labelled at the *HindIII* end using  $[\gamma^{-32}P]$ -ATP and polynucleotide
- 266 kinase. Footprints were done as described by Grainger et al. 54. The in vitro transcription experiments
- were done as described by Savery et al.<sup>55</sup> using the system of Kolb et al.<sup>56</sup>. A Qiagen maxiprep kit
- was used to purify supercoiled pSR plasmid carrying the different promoter inserts. This template (16
- 269 μg ml-1) was pre-incubated with purified H-NS in buffer containing 20 mM Tris pH 7.9, 5 mM
- 270 MgCl2, 500 μM DTT, 50 mM KCl, 100 μg ml-1 BSA, 200 μM ATP, 200 μM GTP, 200 μM CTP, 10
- 271  $\mu$ M UTP with 5  $\mu$ Ci [ $\alpha$ -<sup>32</sup>P]-UTP. The reaction was started by adding purified *E. coli* RNA
- polymerase. Labelled RNA products were analysed on a denaturing polyacrylamide gel. All in vitro
- assays were repeated at least three times in their entirety.
- 274 Growth assays
- 275 Cells lacking H-NS rapidly acquire compensatory mutations<sup>41</sup>. Consequently, reproducible changes in
- 276 growth were only obtained when precautions were taken to minimise this phenomenon. The primary
- 277 precaution was to reduce the number of division cycles that strains passed though during experimental
- 278 setup. Thus, M182 and the hns::kan derivative were taken directly from long-term -80°C storage and
- used immediately to inoculate LB medium. After incubation for several hours at 37°C cells were
- 280 harvested and competency was induced using ice cold CaCl<sub>2</sub>. The cells were then transformed with
- desired plasmids and transformants were isolated on selective agar plates. A colony from each plate
- was suspended in LB medium and aliquots of this were used immediately to inoculate fresh media so

- that growth could be monitored. Cells were grown either in LB medium at 37°C or in M9 minimal
- medium at 30°C. Values shown are from three biological replicates and the experiments were done on
- two separate occasions.
- 286 Western blotting
- To determine relative protein levels in different strains cells were grown in LB media at 37°C.
- 288 Aliquots of the culture were harvested at indicated time points and CFUs determined. Following this
- quantification the same number of cells from each aliquot were resuspended in SDS-PAGE gel
- loading buffer. After heating to 90°C for two minutes we separated proteins present in each lysate
- using SDS-PAGE. The proteins were then transfered to a Hybond-ECL nitrocellulose membrane
- using an Invitrogen XCell II Blot Module. Mouse anti-sera against the  $\sigma^{70}$  and  $\beta$  subunits of RNA
- polymerase (Neoclone) and H-NS (a gift from Jay Hinton) was used to detect the relevant proteins.
- Primary antibody binding was probed with horseradish peroxidise-linked rabbit anti-mouse antisera
- 295 (Sigma-Aldrich A9044). The experiments were done on two separate occasions.
- 296 Standard RNA-seq
- 297 RNA-seq experiments were done in duplicate. E. coli MG1655 and E. coli MG1655 Δhns were grown
- in LB medium at 30°C to an OD<sub>600</sub> of 0.5-0.7. RNA was harvested, RNA-seq libraries were
- 299 constructed and libraries were sequenced as described previously<sup>57</sup>.
- 300 RNA-seq with a spiked in control
- 301 Transcriptome analysis experiments shown were performed in duplicate using *E. coli* MG1655 and *E.*
- 302 coli MG1655  $\Delta hns$ . We also ran the same experiment, again in duplicate, using E. coli M182 and the
- 303 hns::kan derivative. The results were near identical. For each replicate three mid-log phase bacterial
- 304 cultures were prepared. The three cultures were E. coli MG1655, E. coli MG1655 Δhns or Salmonella
- 305 Typhimurium 14028s in LB medium. Before harvesting RNA the number of colony forming units
- 306 (CFUs) per unit volume was determined for each culture by plating dilutions of each culture on
- nutrient agar and counting bacterial colonies. Aliquots of the two E. coli cultures were mixed S.
- 308 Typhimurium cells. The volume of Salmonella cells was normalised to the CFUs for the
- 309 corresponding E. coli culture. This step is crucial because it allows processing artefacts, due to
- differences in lysis efficiency, RNA recovery or cDNA synthesis, to be removed. Thus, in the final
- transcriptome analysis, the number of sequencing reads corresponding to the S. Typhimurium genome
- 312 should be identical for each sample; they were derived from the same number of clonal S.
- 313 Typhimurium cells. Hence, differences can only result from downstream processing. RNA was
- harvested, and RNA-seq libraries were prepared, as described previously<sup>57</sup>. RNA-seq libraries were
- sequenced on am Illumina Hi-Seq 2000 instrument (University at Buffalo, SUNY, Buffalo, NY,
- 316 USA).
- 317 Data normalisation and transcriptome analysis

Our normalisation procedure is based on the addition of a proportional number of *S*. Typhimurium cells to each sample of *E. coli* cells immediately before harvesting RNA. All reads were first mapped to the *E. coli* MG1655 genome using CLC Genomics Workbench (Version 8.0; default parameters except that a perfect match was required). Unmapped reads were mapped to the *S*. Typhimurium 14028s genome (same parameters as above). The number of mapped *S*. Typhimurium reads, for each *E. coli* sample, was used to determine a correction factor for each sample. For example, if Sample A has twice as many *S*. Typhimurium reads as Sample B, the correction factor for Sample A will be twice that for Sample B. Having calculated a correction factor for each sample, we remapped all sequence reads to the *S*. Typhimurium 14028s genome using CLC Genomics Workbench (same parameters as above). Unmapped reads were then mapped to the *E. coli* MG1655 genome using CLC Genomics Workbench (same parameters as above). Total read coverage per gene was calculated using a custom Python script. These values were normalised to the length of the gene, and further normalised using the correction factor (described above). Raw data are available from the ArrayExpress database using accession number E-MTAB-4751.

332 Super resolution microscopy of RNA polymerase

Cell preparation, microscopy, and analysis were performed as described previously 40,58. In brief, we used an endogenous fusion of photoactivatable fluorescent protein PAmCherry, with the  $\beta$ ' subunit of RNA polymerase, encoded by E. coli strain KF26<sup>58</sup>. Glycerol stocks of KF26, and the hns::kan derivative, were used to inoculate fresh Rich Defined Media (RDM, Teknova). When the culture attained an OD<sub>650</sub> value of ~0.2 cells were collected by centrifugation and resuspended. Cells in 1 μl of the suspension were placed on an RDM agarose pad and imaged for 300000 frames at 15 ms exposure on a custom built single-molecule TIRF microscope. For each strain, 9 fields of view were imaged. The experiment was done on 3 separate occasions. Molecules were imaged by photoactivating and localising fluorophores, and joining localisations over multiple frames to obtain trajectories of individual molecules. To measure RNA polymerase mobility, we calculated an apparent diffusion coefficient from the mean squared displacement of trajectories of individual molecules, and used a threshold to distinguish transcriptionally active and promoter bound molecules from the rest of the population. Cell outlines were determined from the brightfield image, and the average intracellular location of RNA polymerase was established from a 2D histogram of the mean trajectory positions relative to the cell outline for all DNA-bound molecules in at least 100 cells. Ter positioning was determined using similar analysis of strain PZ111 carrying a tetO array inserted at Ter, and expressing a TetR-mYpet fusion. The strain was constructed by P1 transduction of tetRmYPet kan, into an AB1157 strain with an array of 240 tetO sequences 50 kb clockwise of dif (ter3)<sup>59</sup>.

Data availability

- 352 The data that support these findings are available from the corresponding author upon request. The
- 353 raw data for RNA-seq experiments are available from the ArrayExpress database using accession
- number E-MTAB-4751. Original gel images are shown in Figure S7.

#### 355 ACKNOWLEDGEMENTS

- 356 This work was funded by Leverhulme Trust project grant (RPG-2013-147) and Wellcome Trust
- 357 Career Development Fellowship (WT085092MA) awarded to D.C.G. Support for J.T.W. was a
- 358 National Institutes of Health Director's New Innovator Award (1DP2OD007188). A.N.K. and M.S.
- were supported by BBSRC grant (BB/N018656/1; to ANK and MS), and a Wellcome Trust
- Investigatorship (110164/Z/15/Z; to ANK). We thank Jay Hinton for the gift of anti-H-NS anti-sera.

#### 361 **CONTRIBUTIONS**

- D.C.G. and J.T.W. designed the study and wrote the manuscript. L.E.L., G.B., S.S.S., A.M.S., R.P.B.,
- and M.S. generated the data and prepared it for publication. M.S. and A.N.K. provided new analytical
- 364 tools and critically discussed the manuscript with D.C.G. and J.T.W. All authors contributed to data
- analysis and interpretation.

#### 366 REFERENCES

- 1. Soucy SM, Huang J, Gogarten JP. 2015. Horizontal gene transfer: building the web of life. *Nat Rev*
- 368 *Genet* **16:** 472-482.
- 2. Doyle M, Fookes M, Ivens A, Mangan MW, Wain J, Dorman CJ. 2007. An H-NS-like stealth
- protein aids horizontal DNA transmission in bacteria. *Science* **315**: 251-252.
- 3. Popa O, Hazkani-Covo E, Landan G, Martin W, Dagan T. 2011. Directed networks reveal genomic
- barriers and DNA repair bypasses to lateral gene transfer among prokaryotes. Genome Res 21: 599-
- 373 609
- 4. Popa O, Dagan T. 2011. Trends and barriers to lateral gene transfer in prokaryotes. Curr Opin
- 375 *Microbiol* **145**: 615-623
- 5. Raghavan R, Kelkar YD, Ochman H. 2012. A selective force favoring increased G+C content in
- 377 bacterial genes. *Proc Natl Acad Sci* **109:** 14504-14507.
- 6. Baltrus DA. 2013. Exploring the costs of horizontal gene transfer. *Trends Ecol Evol* 8: 489-495.
- 7. Dorman CJ. 2007. H-NS, the genome sentinel. *Nat Rev Microbiol.* **5:** 157-61.
- 380 8. Singh K, Milstein JN, Navarre WW. 2016. Xenogeneic Silencing and Its Impact on Bacterial
- 381 Genomes. *Annu Rev Microbiol.* **70:** 199-213.
- 382 9. Navarre WW, Porwollik S, Wang Y, McClelland M, Rosen H, Libby SJ, Fang FC. 2006. Selective
- 383 silencing of foreign DNA with low GC content by the H-NS protein in Salmonella. Science 313: 236-
- 384 238.

- 385 10. Lucchini S, Rowley G, Goldberg MD, Hurd D, Harrison M, Hinton JC. 2006. H-NS mediates the
- silencing of laterally acquired genes in bacteria. *PLoS Pathog* **28:** e81.
- 387 11. Smits WK, Grossman AD. 2010. The transcriptional regulator Rok binds A+T-rich DNA and is
- involved in repression of a mobile genetic element in Bacillus subtilis. *PLoS Genet* **6:** e1001207
- 389 12. Gordon BR, Li Y, Wang L, Sintsova A, van Bakel H, Tian S, Navarre WW, Xia B, Liu J. 2010.
- 390 Lsr2 is a nucleoid-associated protein that targets AT-rich sequences and virulence genes in
- 391 Mycobacterium tuberculosis. *Proc Natl Acad Sci* **107:** 5154-5159.
- 392 13. Dorman CJ. 2014. H-NS-like nucleoid-associated proteins, mobile genetic elements and
- 393 horizontal gene transfer in bacteria. *Plasmid* **75:** 1-11.
- 394 14. Bouffartigues E, Buckle M, Badaut C, Travers A, Rimsky S. 2007. H-NS cooperative binding to
- high-affinity sites in a regulatory element results in transcriptional silencing. Nat Struct Mol Biol 14:
- 396 441-418.
- 15. Gordon BR, Li Y, Cote A, Weirauch MT, Ding P, Hughes TR, Navarre WW, Xia B, Liu J. 2011.
- 398 Structural basis for recognition of AT-rich DNA by unrelated xenogeneic silencing proteins. *Proc*
- 399 Natl Acad Sci 108: 10690-10695.
- 400 16. Arold ST, Leonard PG, Parkinson GN, Ladbury JE. 2010. H-NS forms a superhelical protein
- 401 scaffold for DNA condensation. *Proc Natl Acad Sci* **107:** 15728-15732.
- 402 17. Amit R, Oppenheim AB, Stavans J. 2003. Increased bending rigidity of single DNA molecules by
- 403 H-NS, a temperature and osmolarity sensor. *Biophys J* **84:** 2467-73.
- 404 18. Dame RT, Noom MC, Wuite GJ. 2006. Bacterial chromatin organization by H-NS protein
- 405 unravelled using dual DNA manipulation. *Nature*. **444:** 387-390.
- 406 19. Liu Y, Chen H, Kenney LJ, Yan J. 2010. A divalent switch drives H-NS/DNA-binding
- 407 conformations between stiffening and bridging modes. *Genes Dev.* **24:**339-44.
- 408 20. Landick R, Wade JT, Grainger DC. 2015. H-NS and RNA polymerase: a love-hate relationship?
- 409 *Curr Opin Microbiol* **24:** 53-59.
- 410 21. Winardhi RS, Yan J, Kenney LJ. 2015. H-NS Regulates Gene Expression and Compacts the
- Nucleoid: Insights from Single-Molecule Experiments. *Biophys J.* **109:** 1321-1329.
- 412 22. Dame RT, Wyman C, Wurm R, Wagner R, Goosen N. 2002. J Biol Chem 277: 2146-2150.
- 413 23. Huang Q, Cheng X, Cheung MK, Kiselev SS, Ozoline ON, Kwan HS. 2012. High-density
- transcriptional initiation signals underline genomic islands in bacteria. *PLoS One* **7:** e33759.
- 24. Singh SS and Grainger DC. 2013. H-NS can facilitate specific DNA-binding by RNA polymerase
- in AT-rich gene regulatory regions. *PLoS Genet* **9:** e1003589.
- 417 25. Singh SS, Singh N, Bonocora RP, Fitzgerald DM, Wade JT, Grainger DC. 2014. Widespread
- suppression of intragenic transcription initiation by H NS *Genes Dev* **28:** 214-219.
- 419 26. Lam KN and Charles TC. 2015. Strong spurious transcription likely contributes to DNA insert
- bias in typical metagenomic clone libraries. *Microbiome* **3:** 22.

- 421 27. Kahramanoglou C, Seshasayee AS, Prieto AI, Ibberson D, Schmidt S, Zimmermann J, Benes V,
- 422 Fraser GM, Luscombe NM. 2011. Direct and indirect effects of H-NS and Fis on global gene
- 423 expression control in *Escherichia coli*. *Nucleic Acids Res* **39:** 2073-91.
- 424 28. Chintakayala K, Singh SS, Rossiter AE, Shahapure R, Dame RT, Grainger DC. 2013. E. coli Fis
- protein insulates the *cbpA* gene from uncontrolled transcription. *PLoS Genet* **9:** e1003152.
- 426 29. Wade JT, Castro Roa D, Grainger DC, Hurd D, Busby SJ, Struhl K, Nudler E. 2006. Extensive
- 427 functional overlap between sigma factors in *Escherichia coli*. *Nat Struct Mol Biol*. **13:** 806-814.
- 428 30. Haycocks JR, Sharma P, Stringer AM, Wade JT, Grainger DC. 2015. The molecular basis for
- 429 control of ETEC enterotoxin expression in response to environment and host. PLoS Pathog
- 430 **11:**e1004605.
- 431 31. Piper SE, Mitchell JE, Lee DJ, Busby SJ. 2009. A global view of Escherichia coli Rsd protein and
- 432 its interactions. *Mol Biosyst* **5:** 1943-1947.
- 433 32. Srinivasan R, Scolari VF, Lagomarsino MC, Seshasayee AS. 2015. The genome-scale interplay
- 434 amongst xenogene silencing, stress response and chromosome architecture in Escherichia coli.
- 435 Nucleic Acids Res. 43: 295-308.
- 436 33. Oshima T, Ishikawa S, Kurokawa K, Aiba H, Ogasawara N. 2006. Escherichia coli histone-like
- protein H-NS preferentially binds to horizontally acquired DNA in association with RNA polymerase.
- 438 DNA Res 13: 141-53.
- 439 34. Lovén J, Orlando DA, Sigova AA, Lin CY, Rahl PB, Burge CB, Levens DL, Lee TI, Young RA.
- 440 2012. Revisiting global gene expression analysis. *Cell* **151:** 476-482.
- 35. Lawrence JG, Ochman H. 1998. Molecular archaeology of the Escherichia coli genome. Proc.
- 442 *Natl. Acad. Sci.* USA. **95:** 9413-9417.
- 443 36. Zarei M, Sclavi B, Cosentino Lagomarsino M. 2013. Gene silencing and large-scale domain
- structure of the *E. coli* genome. *Mol Biosyst.* **9:** 758-767.
- 445 37. Dame RT, Kalmykowa OJ, Grainger DC. 2011. Chromosomal macrodomains and associated
- 446 proteins: implications for DNA organization and replication in Gram negative bacteria. PLoS Genet.
- **7:** e1002123.
- 448 38. Junier I, Boccard F, Espéli O. 2014. Polymer modeling of the E. coli genome reveals the
- 449 involvement of locus positioning and macrodomain structuring for the control of chromosome
- 450 conformation and segregation. *Nucleic Acids Res.* **42:** 1461-1473.
- 39. Youngren B, Nielsen HJ, Jun S, Austin S. 2014. The multifork Escherichia coli chromosome is a
- self-duplicating and self-segregating thermodynamic ring polymer. Genes Dev. 28: 71-84.
- 453 40. Stracy M, Lesterlin C, Garza de Leon F, Uphoff S, Zawadzki P, Kapanidis AN. 2015. Live-cell
- superresolution microscopy reveals the organization of RNA polymerase in the bacterial nucleoid.
- 455 *Proc Natl Acad Sci* USA. **112:** E4390-9.
- 41. Ali SS, Soo J, Rao C, Leung AS, Ngai DH, Ensminger AW, Navarre WW. 2014. Silencing by H-
- NS potentiated the evolution of *Salmonella*. *PLoS Pathog* **10**: e1004500.

- 458 42. Lee DJ, Minchin SD, Busby SJ. 2012. Activating transcription in bacteria. Annu Rev Microbiol.
- **459 66:** 125-152.
- 460 43. Miroslavova NS and Busby SJ. 2006. Investigations of the modular structure of bacterial
- promoters. *Biochem Soc Symp* **73:** 1-10.
- 462 44. Castang S, McManus HR, Turner, KH, Dove, SL. 2008. H-NS family members function
- 463 coordinately in an opportunistic pathogen. *Proc. Natl. Acad. Sci.* USA **105**: 18947-18952.
- 464 45. Li C, Wally H, Miller SJ, Lu CD. 2009. The Multifaceted Proteins MvaT and MvaU, Members of
- 465 the H-NS Family, Control Arginine Metabolism, Pyocyanin Synthesis, and Prophage Activation in
- 466 Pseudomonas aeruginosa PAO1. J. Bacteriol. 191: 6211-6218.
- 46. Kotlajich MV, Hron DR, Boudreau BA, Sun Z, Lyubchenko YL, Landick R. 2015. Bridged
- 468 filaments of histone-like nucleoid structuring protein pause RNA polymerase and aid termination in
- 469 bacteria. *Elife* **4:** e04970.
- 47. Page L, Griffiths L, Cole JA. 1990. Different physiological roles of two independent pathways for
- 471 nitrite reduction to ammonia by enteric bacteria. *Arch Microbiol* **154:** 349-354.
- 48. Keseler IM, Mackie A, Peralta-Gil M, Santos-Zavaleta A, Gama-Castro S, Bonavides-Martínez C,
- 473 Fulcher C, Huerta AM, Kothari A, Krummenacker M, et al. 2013. EcoCyc: fusing model organism
- databases with systems biology. *Nucleic Acids Res* **41:** D605-12.
- 475 49. Lee, DJ, Bingle LE, Heurlier K, Pallen MJ, Penn CW, Busby SJ, Hobman JL. 2009. Gene
- doctoring: a method for recombineering in laboratory and pathogenic Escherichia coli strains. BMC
- 477 *Microbiol* **9:** 252.
- 478 50. Rhodius VA, Busby SJ. 2000. Interactions between activating region 3 of the Escherichia coli
- 479 cyclic AMP receptor protein and region 4 of the RNA polymerase sigma 70 subunit: application of
- suppression genetics. J Mol Biol 299: 311-324.
- 481 51. Lodge J, Fear J, Busby S, Gunasekaran P, Kamini NR. 1992. Broad host range plasmids carrying
- 482 the Escherichia coli lactose and galactose operons. FEMS Microbiol Lett. 74: 271-276.
- 483 52. Miller J 1972. Experiments in Molecular Genetics. Cold Spring Harbor, NY: Cold Spring Harbor
- 484 Laboratory Press.
- 485 53. Grainger DC, Goldberg MD, Lee DJ, Busby SJ. 2008. Selective repression by Fis and H-NS at the
- 486 Escherichia coli dps promoter. Mol Microbiol **68:** 1366-1377.
- 487 54. Grainger DC, Belyaeva TA, Lee DJ, Hyde EI, Busby SJ. 2004. Transcription activation at the
- 488 Escherichia coli melAB promoter: interactions of MelR with the C-terminal domain of the RNA
- polymerase alpha subunit. *Mol Microbiol* **51:** 1311-1320.
- 490 55. Savery NJ, Lloyd GS, Kainz M, Gaal T, Ross W, Ebright RH, Gourse RL, Busby SJ. et al. 1998.
- 491 Transcription activation at Class II CRP-dependent promoters: identification of determinants in the C-
- terminal domain of the RNA polymerase alpha subunit. *EMBO J* **17:** 3439-3447.
- 493 56. Kolb A, Kotlarz D, Kusano S, Ishihama A 1995. Selectivity of the Escherichia coli RNA
- 494 polymerase E sigma 38 for overlapping promoters and ability to support CRP activation. *Nucleic*
- 495 Acids Res 23: 819-826.

- 496 57. Stringer AM, Currenti S, Bonocora RP, Baranowski C, Petrone BL, Palumbo MJ, Reilly AA,
- Zhang Z, Erill I, Wade JT. 2014. Genome-scale analyses of *Escherichia coli* and Salmonella enterica
- 498 AraC reveal noncanonical targets and an expanded core regulon. *J Bacteriol* **196:** 660-671.
- 499 58. Endesfelder U, Finan K, Holden SJ, Cook PR, Kapanidis AN, Heilemann M. 2013. Multiscale
- spatial organization of RNA polymerase in *Escherichia coli. Biophys J.* **105:** 172-181.
- 59. Zawadzki P, Stracy M, Ginda K, Zawadzka K, Lesterlin C, Kapanidis AN, Sherratt DJ. 2015. The
- 502 Localization and Action of Topoisomerase IV in Escherichia coli Chromosome Segregation Is
- Coordinated by the SMC Complex, MukBEF. *Cell Rep.* **13:** 2587-2596.

# 504505 **FIGURES**

#### 506 Figure 1: Characterisation of the *yccE* locus.

- a) **Genomic context of** *yccE* and its promoter. The panel shows *yccE*, and surrounding genes, alongside data describing H-NS binding (ChIP-seq<sup>27</sup>) and RNA abundance (standard RNA-seq; this
- work, done in duplicate). Data are representative.
- 510 **b) Sequence of the**  $yccE\Delta 200$  **DNA fragment containing** PyccE**.** The PyccE -10 and -35 elements
- are in bold and underlined. A consensus  $\sigma^{32}$  promoter sequence is in grey for comparison. Mutations
- 512 made to disrupt sequence elements are in red. Transcription can initiate at adjacent nucleotides. These
- are labelled (+1) and are highlighted by a bent arrow.
- 514 c) Analysis of transcripts generated from PyccE in vitro. The gel image shows transcripts
- generated by RNA polymerase, associated with either  $\sigma^{70}$  or  $\sigma^{32}$ , from pSR plasmid DNA templates.
- The schematic diagrams above the gel image represent the native cloning site of pSR (left hand side)
- or derivatives containing a PyccE insert (right hand side). The different PyccE containing DNA
- fragments inserted are indicated below the gel image in parenthesis. PyccE derived transcripts
- manifest as a 107/106 nucleotide (nt) doublet. The 108/107 nt RNA-I transcript is derived from the
- 520 plasmid replication origin. The experiment was done three times. Data are representative.
- **d)** Effect of PyccE mutation in vivo. The graph shows LacZ activity data obtained from E. coli
- JCB387 cells carrying different yccEΔ200 derivatives cloned in pRW50. Assays were done in
- 523 triplicate and error bars show standard deviation from the mean.
- e) Induction of yccE transcription in the absence of H-NS does not require PyccE in vivo. The
- panel illustrates a series of yccE::lacZ fusions labelled i-iv. Genes are shown as block arrows and
- 526 PyccE is shown as a bent line arrow. The β-galactosidase activity was measured in lysates of M182
- 527 (grey bars) and M182hns::kan cells (open bars). Assays were done in triplicate and error bars show
- standard deviation from the mean.

529 530

#### Figure 2: H-NS represses intragenic yccE transcription and associated fitness costs

- a) Identification of intragenic yccE promoters. The data are  $\beta$ -galactosidase activities driven by
- short intragenic *yccE* DNA fragments in strain JCB387. The bars align with the location of the DNA fragment relative to *yccE* and show sense (upper) and antisense (lower) transcription. Bars labelled
- "a"-"k" have at least 2-fold over background activity (empty pRW50; shown by dashed line). The
- black bar represents the canonical promoter PyccE. Note that, two DNA fragments resisted cloning.
- Hence, 19 of the 21 potential promoters were tested. Assays were done in triplicate. Error bars show
- standard deviation from the mean.
- b) Transcription can initiate at multiple sites within yccE in vitro. Gel image showing RNA
- generated in vitro separated by denaturing gel electrophoresis. DNA templates, with the yccE gene
- cloned upstream of the  $\lambda oop$  terminator in plasmid pSR, are illustrated above the gel. Transcripts
- 541 generated by RNA polymerase (400 nM) with empty pSR plasmid (lane 1) are highlighted by a black
- dashed line. Transcripts initiating within yccE in the forward (lanes 2-5) or reverse (lanes 6-9)
- orientation are highlighted by a blue dashed line. The control RNA-I transcripts are highlighted by a
- grey dashed line. H-NS was added at concentrations of 0.8, 1.5, or 3.0 uM. The experiment, done
- 545 three times, is representative.

c) Mutation of promoters within yccE prevents induction in  $\Delta hns$  cells. The lower illustrations show yccE (blue arrows) cloned upstream of lacZ (red arrow). A solid blue arrow represents wild type yccE whereas open arrows indicate yccE with mutated intragenic promoter -10 elements. For each lacZ fusion,  $\beta$ -galactosidase activity was measured in lysates of M182 (grey bars) and M182hns::kan cells (open bars). Assays were done in triplicate and error bars show standard deviation from the mean.

**d,e)** The fitness cost of *yccE* is reduced when intragenic promoters are mutated. The figure illustrates changes in culture OD<sub>650</sub> following inoculation of LB medium. The inoculum was M182 (solid line) or M182*hns*::kan (dashed line) transformed with the pSR plasmid carrying d) wild type *yccE* or e) *yccE* with internal promoter -10 elements mutated. Cells were grown at 37°C. The experiment was done in triplicate. Error bars show standard deviation from the mean.

#### Figure 3: H-NS represses intragenic transcription and associated fitness costs at many loci.

- a) Transcription initiation within the coding regions of H-NS target genes in vitro. An in vitro transcription assay using different AT-rich genes, cloned upstream of the  $\lambda oop$  terminator in plasmid pSR, as a template. The different DNA constructs are illustrated above the gel. The cloned genes have an AT-content of 65% (yfdF), 63% (ykgH), 63% (yjgN) and 68% (yjgL). For each cloned gene a solid arrow represents the wild type DNA sequence whereas an open arrow is a derivative where intragenic promoter -10 elements have point mutations. Note that the fepA gene was used as a control and has an AT-content of 55%. The positions of transcripts generated by RNA polymerase (400 nM) from the fepE control (lane 1) or the other cloned genes (lanes 2-9) are labelled. The  $in\ vitro$  transcription assays were run on three separate occasions. Data are representative.
- b) Increased transcription in cells lacking H-NS frequently requires intragenic promoters in vivo. The panel illustrates a series of DNA constructs where different gene coding regions have been cloned upstream of lacZ (red arrow). For each cloned gene a solid arrow represents the wild type DNA sequence whereas an open arrow is a derivative where intragenic promoter -10 elements have point mutations. The cloned genes have an AT-content of 65% (yfdF), 63% (ykgH), 63% (yjgN) and 68% (yjgL). Note that the fepA gene is used as a control and has an AT-content of 55%. For each lacZ fusion  $\beta$ -galactosidase activity was measured in lysates of M182 (grey bars) and M182 $\Delta hns$  (open bars) cells. Assays were done in triplicate and error bars show standard deviation from the mean.
- **c,d)** The toxicity of many AT-rich genes is a consequence of spurious intragenic transcription. The figure illustrates growth of M182 (solid line) or M182*hns*::kan (dashed line) cells transformed with the pSR plasmid carrying different AT-rich genes. Panel c) shows wild type gene derivatives and d) shows derivatives with internal promoter -10 elements mutated (open arrows). Experiments were done using M9 minimal media at 30°C. The experiment was done in triplicate and error bars show standard deviation from the mean.

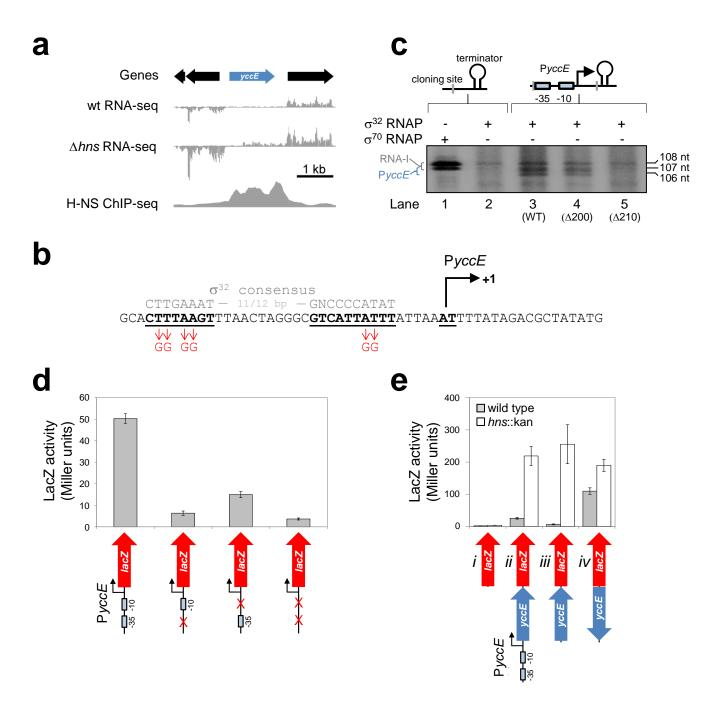
#### Figure 4: Most transcription is uniformly downregulated in cells lacking H-NS.

- **a,b) Most transcription is uniformly downregulated in cells lacking H-NS.** a) the plot illustrates changes in global transcription caused by loss of H-NS. Data points represent H-NS bound (red) and unbound (black) genes. Genes with unaltered transcription should fall on the diagonal blue line. Data are from duplicate RNA-seq experiments. b) The basally expressed *fad* genes whose transcription is reduced in the absence of H-NS. Genes bound by H-NS are in red and other genes are black. Graphs show H-NS binding<sup>27</sup> and RNA abundance (RNA-seq with spiked in control; this work). Data are representative.
- c) RNA polymerase is redistributed in cells lacking H-NS. RNA polymerase distribution in wild type (top) and *hns*::kan cells (middle). Each heat map shows the average position of DNA-bound (i.e. transcribing or interacting with a promoter) RNA polymerase molecules within the cell. The bottom panelshows the average position of Ter as determined by visualising a TetR-mYpet fusion bound at an array of Ter proximal *tetO* sequences. Each distribution was generated from 100 cells between 3.5 and 4.5 µm in length. Each square is 1/624 of total cell area.
- d) The  $\sigma^{70}$  G424D mutation hinders constitutive but not activator dependent NM501 promoter activity in vitro. KMnO<sub>4</sub> footprinting reactions analysed on a denaturing polyacrylamide gel. Bands are indicative of open complex near the transcription start site (+1). RNA polymerase added at

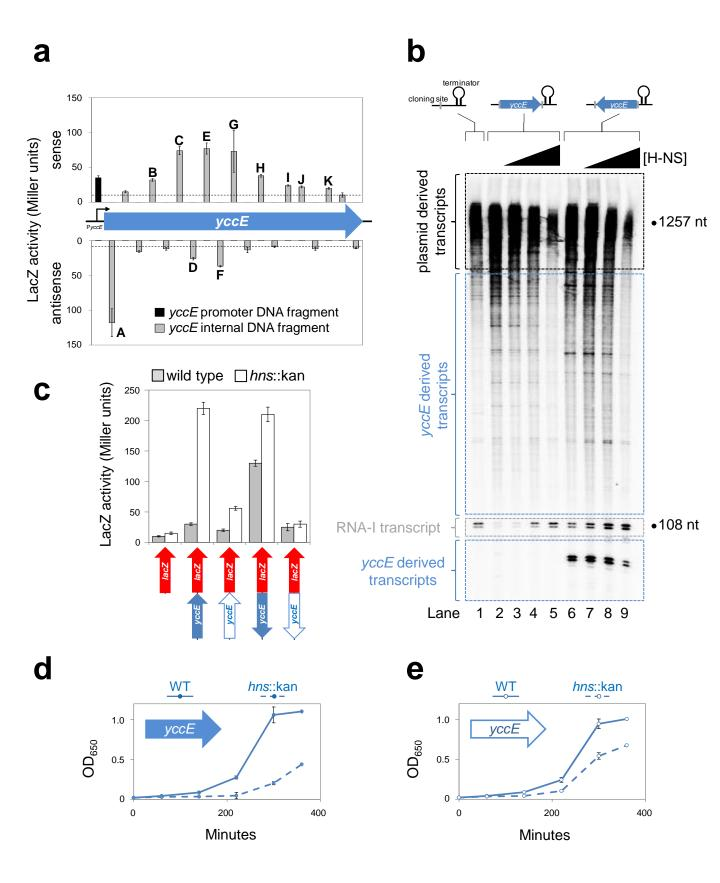
concentrations of 200, 250, 300 or 350 nM and CRP was 1.0  $\mu$ M. The experiment, done three times, is representative.

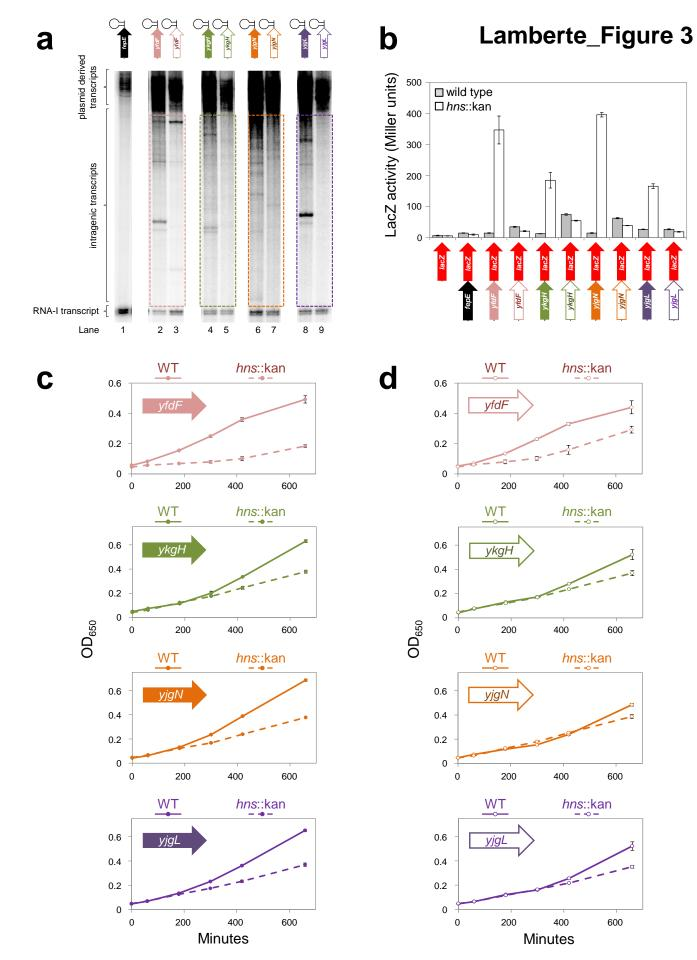
 e,f) The  $\sigma^{70}$  G424D mutation hinders constitutive but not activator dependent promoter activity *in vivo*. Different promoter DNA fragments were cloned upstream of *lacZ* (red arrow). For each promoter the location of key DNA sequence elements is represented by a box. In each case, the box is coloured according to the relationship between the DNA sequence and the consensus sequence for that element: perfect (dark blue), imperfect (pale blue) or completely absent (white). For each *lacZ* fusion  $\beta$ -galactosidase activity was measured in lysates of JCB387*rpoD*::kan carrying pVR $\sigma$  (white bars) or pVR $\sigma^{G424D}$  (black bars). The experiment was done in triplicate. Error bars show standard deviation from the mean.

# Lamberte\_Figure 1



# Lamberte\_Figure 2





# Lamberte\_Figure 4

